

Structural transition of hexagonal tube to rocksalt for $(\text{MgO})_{3n}$, $2 \leq n \leq 10$

Ruibin Dong, Xiaoshuang Chen,^{a)} Xiaofang Wang, and Wei Lu^{a)}

National Laboratory for Infrared Physics, Shanghai Institute of Technical Physics, Chinese Academy of Sciences, Shanghai 200083, People's Republic of China

(Received 8 April 2008; accepted 18 June 2008; published online 28 July 2008)

The structures of $(\text{MgO})_{3n}$ ($2 \leq n \leq 10$) clusters are studied using density functional theory (DFT). The starting structures are generated from empirical genetic algorithm simulations. The lowest-energy structures of $(\text{MgO})_{3n}$ are then obtained from a number of structural isomers by using DFT optimization. It is found that when $n \leq 5$ hexagonal tube is the most stable structure, and when $n \geq 6$ (except 7) the rocksaltlike structure is favored, which is the same as that of the bulk. The $n=7$ is an interesting case, where the structure again is the hexagonal tube as the most stable structure. However, from the second order difference of the average atomization energy, we find that the $n=7$ case is thermodynamically unstable with respect to disproportionation to the smaller and larger clusters. The result may be the reason that it is not observed in the experiment. Therefore, we can conclude that the geometry transition really takes place at $n=6$. The rocksalt is the most stable structure for a large range of n numbers, from the $(\text{MgO})_{3 \times 6}$ cluster to bulk magnesium oxide. The result is different from Wilson's previous prediction because of the use of the ionic potential.

© 2008 American Institute of Physics. [DOI: 10.1063/1.2956508]

I. INTRODUCTION

For the past two decades, magnesium oxide (MgO) of different scales and dimensions, as an important functional material, has been widely studied both experimentally^{1,2} and theoretically.³⁻⁷ Its powder is considered as a kind of dopants to form high-temperature superconductor thick films^{8,9} and also as a very important metal oxide for use in catalysis.^{10,11} Bulk MgO could be a very good substrate for growing thin films or other materials. Since the studies of surface properties and nanostructures of MgO, some interesting problems have been presented. Which structures are there for different scale and dimension MgO? Do the nanostructures have the same structure as the bulk? What are the subunits for the nanostructures? One way to understand these issues is to study the size dependence of clusters, which are considered as the intermediate size between individual atoms and bulk. Actually lots of jobs have been done for clusters.¹²⁻¹⁶ As the clusters are aggregates of atoms, the clusters can serve as a bridge for understanding how MgO evolves from atoms to bulk.

As in the early 1990s, the beam experiment has shown some magic number clusters with great stabilities, as $(\text{MgO})_{3n}$ at $n=(2-6, 8-10)$.^{1,2} Many theoretical studies have also been done to investigate the structures for $(\text{MgO})_m$. Some of them have used the sophisticated model potentials, such as the Born-Mayer potential^{17,1} and compressible-ion interaction model (CIM).¹⁸ Roberts and Johnston showed some interesting structures for the clusters $(\text{MgO})_m$.¹⁷ In Wilson's work,¹⁸ a structural transition of the MgO clusters has been indicated and a cubiclike structure is formed as the clusters containing more than 60 atoms.¹⁹⁻²⁶ However, first-

principles study has been carried out only for small $(\text{MgO})_m$ clusters ($m \leq 15$).²⁷⁻³³ It is well known that the CIM or the Born-Mayer potential is not precise enough to predict the most stable structures of the clusters where the isomers exist with a little difference in atomization energy (AE). Therefore, the most stable structure for medium sized clusters and the rearrangement from small unit structures into the bulk-like rocksalt lattice in MgO are still open questions.

In this paper, by using density-functional theory (DFT): The equilibrium structures of $(\text{MgO})_{3n}$ ($n=2-10$) clusters are determined from a number of isomers generated by genetic algorithm (GA) simulation based on Born-Mayer potential.¹⁷ Our results have well shown the structural transition (from hexagonal tube to rocksalt) as the cluster size gets large.

The paper is organized as follows. In Sec. II we introduce the methods we used to investigate the problem. In Sec. III we explore the results and some discussion according to the results. Conclusions are outlined in Sec. IV.

II. METHODS

The ground state structure is one of the most fundamental issues in cluster physics. The most commonly used strategy in searching the most stable structures of small clusters is the simulated annealing (SA) scheme based on DFT calculations, but SA is really hard to do for clusters with the number of atoms being greater than 10. Following the study of Ref. 17, we use an unbiased global search of the optimal cluster isomers from GA (Refs. 34-36) based on Born-Mayer potential. In combining with DFT, the global optimal configuration of the structure could be achieved. GA is a powerful global optimal scheme based on the principle of natural evolution.³⁷ We use GA to generate isomers for $(\text{MgO})_{3n}$ ($n=2-10$) at each n with the Born-Mayer inter-

^{a)}Authors to whom correspondence should be addressed. Electronic addresses: xschen@mail.sitp.ac.cn and luwei@mail.sitp.ac.cn.

atomic potentials following earlier study on magnesium oxide clusters in Ref. 17. To effectively represent the range of structural preferences due to ionic polarization, the charge of the clusters $\text{Mg}^{q+}\text{O}^{q-}(q)$ is varied between 1 and 1.5 with the intervals of 0.1 as in Ref. 38. The main process of employing GA to find the isomers of clusters is as follows. For each n and q of $(\text{MgO})_{3n}$, starting with a “population” of candidate structures generated randomly, we use a local optimal-searching method to find the nearest maximum for every candidate structure. Then the local maximum energies are considered as the criteria of “fitness” (the probability to be chosen as a parent to generate the next generation, for an isomer, the larger atomization energy it has the larger probability to be chosen) for the population. Based on the fitness of the population, two structures are selected as the “parents.” We “mate” these two parents, and then we get a new isomer. If the new one has higher atomization energy than any one of the candidates we generate as the population, the old one who has lower energy would be replaced by the new one, and we get the next generation. The process repeats at proper steps, and finally only the optimal isomers of the structures exist. The processes are also similar to Ref. 17. After we get the isomers generated by the GA, the electronic structural calculations on $(\text{MgO})_{3n}$ ($n=2-10$) clusters are performed by using the DMOL package³⁹ based on DFT. The all electrons and a double numerical basis are chosen. The exchange correlation has been treated with the generalized gradient approximation (GGA) as described by Perdew and Wang.^{40,41} Self-consistent calculations are carried out with a convergence criterion of 10^{-5} a.u. on the total energy. Geometry optimizations are performed with the Broyden-Fletcher-Goldfarb-Shanno algorithm. We use a convergence criterion of 10^{-3} a.u. on the gradient and displacement, and 10^{-5} a.u. on the total energy in the geometry optimization.

III. RESULTS AND DISCUSSION

We present the calculated optimal structures for different size n . For each cluster size, we obtain not only the most stable structure but also the isomers with small total energy

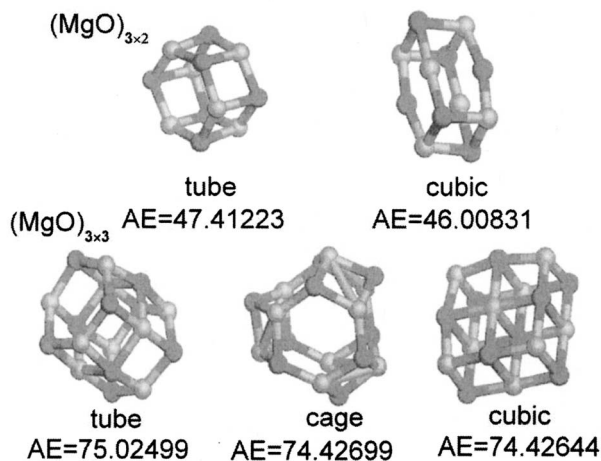


FIG. 1. The calculated ground state geometries and some isomers for $(\text{MgO})_{3n}$ with $n=2$ and 3. The total AE in eV is listed. White ball indicates Mg atom, while gray ball indicates O atom.

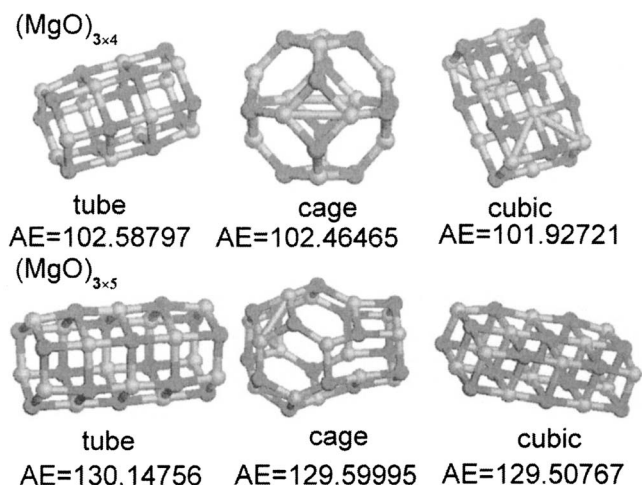


FIG. 2. The calculated ground state geometries and some isomers for $(\text{MgO})_{3n}$ and their AEs (eV) with $n=4$ and 5.

differences compared to the most stable one. Figures 1–5 show the most stable structure and some isomers for each size of $(\text{MgO})_{3n}$ ($n=2-10$). It can be seen that for $(\text{MgO})_{3n}$ the hexagonal tube is the most stable structure for $n=2-5$ and 7, while the rocksalt structure is the most stable structure for $n=6, 8-10$. In order to understand the geometry evolution clearly, we calculate the AE, which is defined as required energy to break a $(\text{MgO})_m$ cluster into separated Mg and O atoms. The AE is calculated using the equation

$$\text{AE} = mE(\text{Mg}) + mE(\text{O}) - E((\text{MgO})_m). \quad (1)$$

In Eq. (1), in calculating the AE, we consider the effect of basis set superposition error. We use the counterpoise method to calculate the AE for every m . The results for $m=3n$ ($n=2-10$) are shown in Fig. 8. We focus on the cluster size for $3n$ because they are the magic numbers in these sizes from the observation of the experiment. In our calculation, using the same method, we predict the most stable structures of $(\text{MgO})_m$ ($1 \leq m \leq 30$), respectively [naturally the $(\text{MgO})_{3n}$ ($n=2-10$) are also included], as shown in Fig. 6 [except the previous results $(\text{MgO})_{3n}$ ($n=2-10$)].

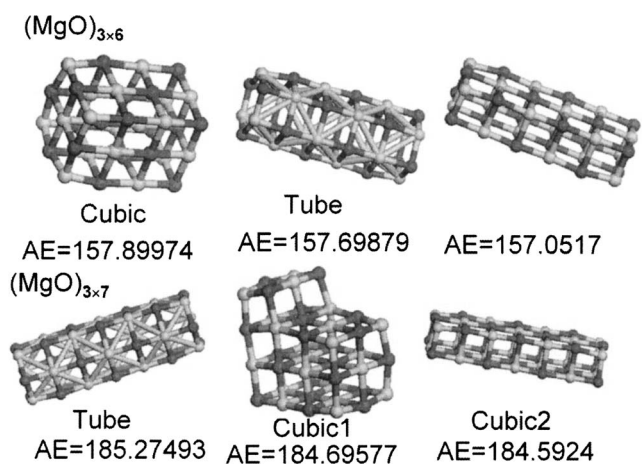


FIG. 3. The calculated ground state geometries and some isomers for $(\text{MgO})_{3n}$ and their AEs (eV) with $n=6$ and 7.

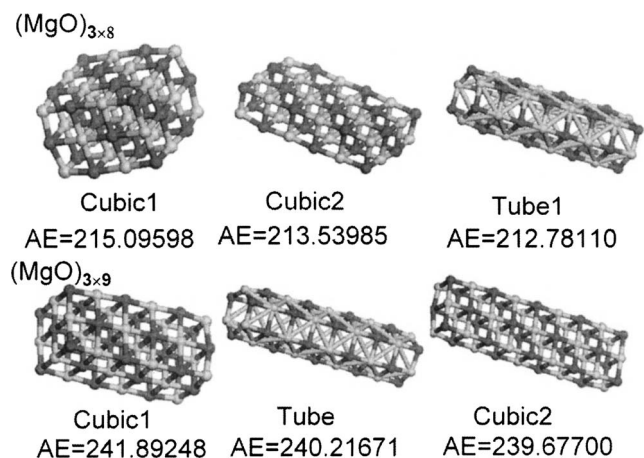


FIG. 4. The calculated ground state geometries and some isomers for (MgO)_{3n} and their AEs (eV) with $n=8$ and 9.

Then we calculate the second order difference $\Delta_2 E_m$ of average AE of the most stable structure of (MgO)_m for ($2 \leq m \leq 29$) as follows:

$$\Delta_2 E_m = 2E((\text{MgO})_m) - E((\text{MgO})_{m+1}) - E((\text{MgO})_{m-1}). \quad (2)$$

As shown in Fig. 7, we can find that the $\Delta_2 E_m$ for (MgO)_m at $m=3 \times 2, 3 \times 3, 3 \times 4, 3 \times 5, 3 \times 6, 3 \times 8,$ and 3×9 are both larger than zero. The result shows that there is greater thermodynamic stability. However; for $m=21$ the $\Delta_2 E_m$ is negative, indicating that the structure is thermodynamically unstable with respect to disproportionation to the smaller and larger clusters. The result agrees well with that of the experiment.⁵ It also indicates that in our calculation (MgO)_{3n} ($n=2-6, 8, 9$) are really outstanding.

From Figs. 1-5, it can be found that the clusters are made of two basic subunits, the square ring of (MgO)₂ and the hexagonal ring of (MgO)₃. For example, as shown in Fig. 1, the cagelike isomer for (MgO)_{3×3} has five square

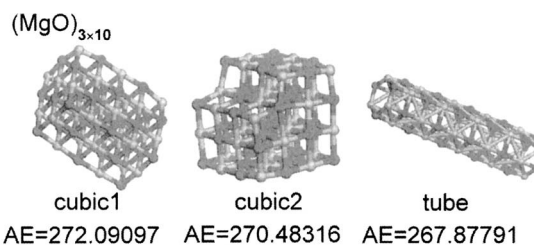


FIG. 5. The calculated ground state geometries and some isomers for (MgO)_{3n} and their AEs (eV) with $n=10$.

rings and six hexagonal rings. In Fig. 2 the cagelike isomer for (MgO)_{3×5} has 12 square rings and 7 hexagonal rings. Similar subunits have also been found for medium sized metal oxide clusters and metal nitride clusters.⁴²⁻⁵⁰ When the cluster size is small, the hexagonal ring is favored. As the cluster gets large, the square rings get more stable. Because the cluster size gets large, the polarization of ions becomes more serious. Therefore, the charge of each atom becomes small, and the structures of clusters change from hollow cages to cuboids with higher coordinates.¹⁷

For (MgO)_{3n} cluster, when $n=2$ the AE of the rocksalt structure is about 0.4 eV lower than the case of the hexagonal tube. The AEs of the other isomers are not shown here because they have very low value. For $n=3$, except for the hexagonal-tube and cubiclke structures, there exists a cagelike structure. For $n=4$, the structures agree well with Carrasco's prediction.³⁸ In the present calculations, the results of small (MgO)_{3n} clusters are consistent with previous DFT calculations.²⁷ For $n=5$, the cagelike isomer is very

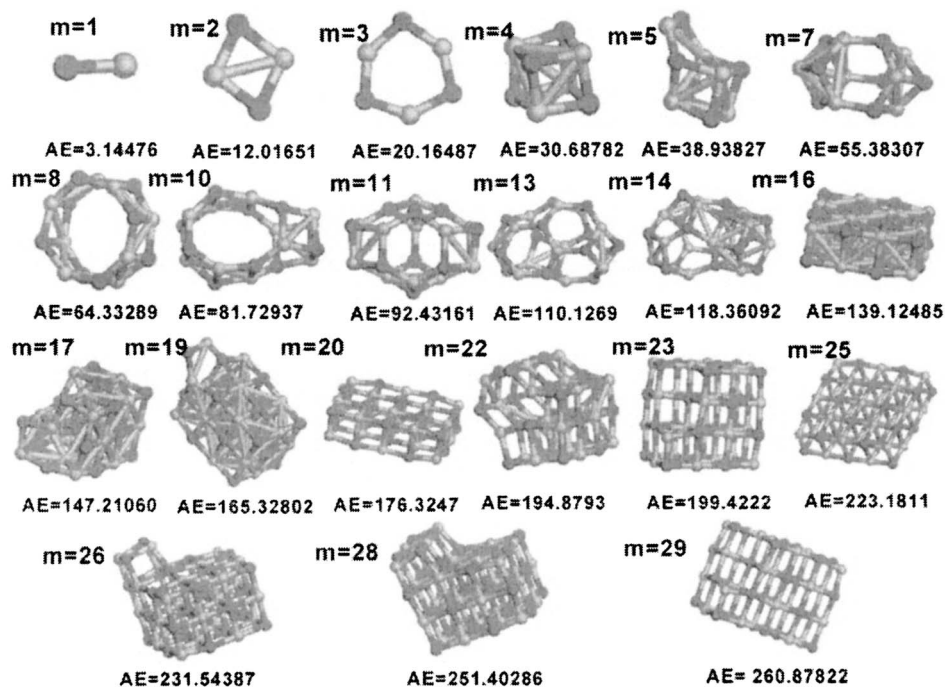


FIG. 6. The calculated ground state geometries for (MgO)_n $1 \leq n \leq 30$, except for the structures that appeared in Figs. 1-5.

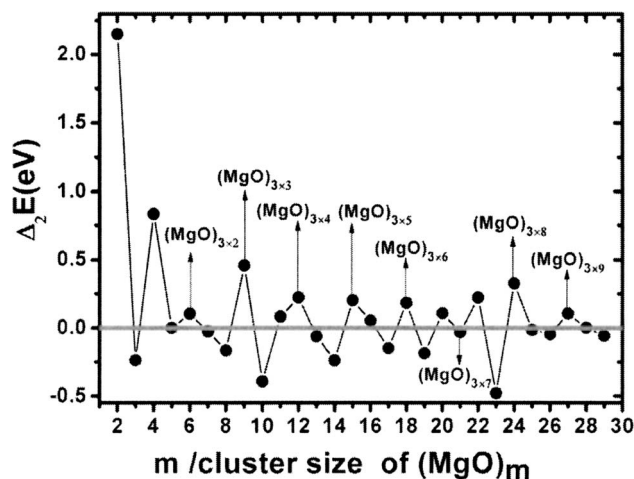


FIG. 7. The $\Delta_2 E_n$ (eV) of $(\text{MgO})_n$, $2 \leq n \leq 29$.

interesting. It is made of a perfect cage of $(\text{MgO})_{12}$ and a cube, in good agreement with Carrasco's predictions.³⁸ It is indicated that a perfect $(\text{MgO})_{12}$ cage may be a building block for bulk structure. For $n=6$, the rocksalt structure is more stable than the hexagonal-tube structure, and the transition happens at such a size. The $n=7$ case is another interesting case. In fact, it has not been observed in the cluster beam experiment. In the present calculations, the hexagonal tube is the most stable structure for $n=7$, while for $n=6$ and $n=8$, the rocksalt structure is favored. It is obvious that the stable structure of the $n=7$ case is different from that of the $n=6$ and 8 cases. From the second order difference of the average AE, we also have found that the structure of the $n=7$ case is thermodynamically unstable with respect to disproportionation to the smaller and larger clusters. Here, we can think that transition occurs at $n=6$ case because of the unstable structure for $n=7$. The result is different from previous Wilson's prediction¹⁸ because of using the CIM ionic potential. Furthermore, as the cluster size gets large, the clusters get more regular and more periodic. For $n \geq 6$, other isomers except the hexagonal-tube or the rocksalt structures have too low AE. These isomers are not shown here because

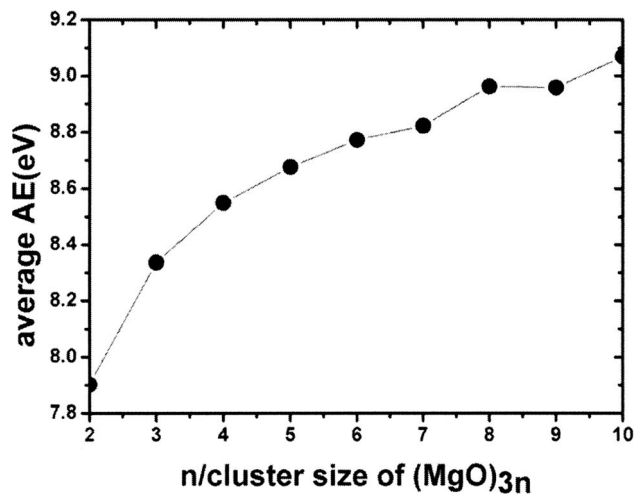


FIG. 8. The average AE (eV) of the ground state geometries as a function of the cluster size.

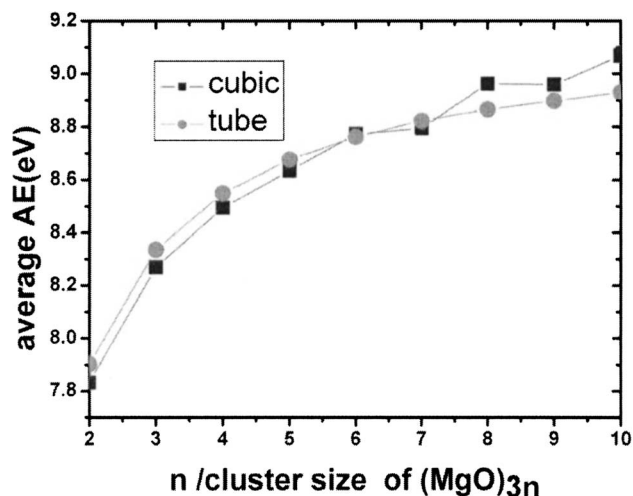


FIG. 9. The average AE (eV) of the hexagonal-tube structure and the rock-salt structure as a function of the cluster size.

of the unstable structures. The AE values of the most stable clusters of $(\text{MgO})_{3n}$ ($n=2-10$) are presented in Fig. 8. As the cluster size gets large, the AE increases rapidly for $3 \leq n \leq 7$. It is found that when n goes from 6 to 7, a jump of AE is shown. However, when n goes from 7 to 8, another jump occurs, where the geometry structure jumps back to that of $n=6$ case. At the same time, the structure is unstable for $n=7$. Therefore, we can say that such behavior can be related to the obtained structure transition around $n=6$. The average AE values of the isomers for the rocksalt and the hexagonal-tube structures at all sizes are shown in Fig. 9. The geometry transition can be found clearly. Also in Fig. 8 we can find that the AE of the hexagonal-tube structure is a little bigger than the rocksalt structure, although the hexagonal tube is a more stable structure for small size clusters.

IV. CONCLUSIONS

The lowest-energy geometries and the AEs of $(\text{MgO})_{3n}$ ($n=2-10$) clusters have been obtained by DFT-GGA calculations in combination with a GA. The main findings are summarized as follows.

- For MgO material, the most stable structure is the rocksalt for a large range of n number from the $(\text{MgO})_{3 \times 6}$ cluster to bulk. It can be concluded that the $(\text{MgO})_{3n}$ clusters follow a rocksalt growth evolution starting from $n=6$. The hexagonal-tube structure is dominant in the range of $n=2-5$. For the first time, we show a geometry transition for $(\text{MgO})_{3n}$ clusters with $n=6$.
- The clusters are made of subunits of $(\text{MgO})_2$ and $(\text{MgO})_3$. The hexagonal-tube structure is the most stable with $n \leq 6$.

ACKNOWLEDGMENTS

This work was supported in part by a grant from the State Key Program for Basic Research of China (2007CB613206), National Natural Science Foundation of China (10725418, 10734090, and 60576068), Creative Group (60221502), and the Knowledge Innovation Program

of the Chinese Academy of Sciences. We are also grateful to the Shanghai Super-Computer Center.

- ¹P. J. Ziemann and A. W. Castleman, Jr., *J. Chem. Phys.* **94**, 718 (1991).
- ²W. A. Saunders, *Phys. Rev. B* **37**, 6583 (1988).
- ³A. Aguado and P. A. Madden, *Phys. Rev. Lett.* **94**, 068501 (2005).
- ⁴P. Yang and C. M. Lieber, *Science* **273**, 1836 (1996).
- ⁵G. W. Wagner and P. W. Bartram, *J. Phys. Chem. B* **103**, 3225 (1999).
- ⁶Q. Yang, J. Sha, and L. Wang, *Nanotechnology* **15**, 1004 (2004).
- ⁷A. Aguado, *Phys. Rev. Lett.* **94**, 068301 (2005).
- ⁸A. Bhargava, J. A. Alarco, I. D. R. Mackinnon, and D. Page, *Mater. Lett.* **34**, 133 (1998).
- ⁹Y. S. Yuan, M. S. Wong, and S. S. Wang, *J. Mater. Res.* **11**, 8 (1996).
- ¹⁰S. H. C. Liang and I. D. Gay, *J. Catal.* **101**, 293 (1986).
- ¹¹H. Tsuji, F. Yagi, H. Hattori, and H. Kita, *J. Catal.* **148**, 759 (1994).
- ¹²V. Kumar and Y. Kawazoe, *Phys. Rev. B* **75**, 155425 (2007).
- ¹³V. Kumar and Y. Kawazoe, *Phys. Rev. Lett.* **87**, 045503 (2001).
- ¹⁴M. C. Fallis, M. S. Daw, and C. Y. Fong, *Phys. Rev. B* **51**, 7817 (1995).
- ¹⁵R. B. King, T. Heine, and C. Corminboeuf, *J. Am. Chem. Soc.* **126**, 430 (2004).
- ¹⁶Y. Xie, H. F. Schaefer III, and R. B. King, *J. Am. Chem. Soc.* **127**, 2818 (2005).
- ¹⁷C. Roberts and R. L. Johnston, *Phys. Chem. Chem. Phys.* **3**, 5024 (2001).
- ¹⁸M. Wilson, *J. Phys. Chem. B* **101**, 4917 (1997).
- ¹⁹T. M. Köhler, H. P. Gail, and E. Sedlmayr, *Astron. Astrophys.* **320**, 553 (1997).
- ²⁰S. Moukouri and C. Noguera, *Z. Phys. D: At., Mol. Clusters* **24**, 71 (1992).
- ²¹S. Moukouri and C. Noguera, *Z. Phys. D: At., Mol. Clusters* **27**, 79 (1993).
- ²²M. J. Malliavin and C. Coudray, *J. Chem. Phys.* **106**, 2323 (1997).
- ²³J. M. Recio, R. Pandey, A. Ayuela, and A. B. Kunz, *J. Chem. Phys.* **98**, 4783 (1993).
- ²⁴E. de la Puente, A. Aguado, A. Ayuela, and J. M. Lopez, *Phys. Rev. B* **56**, 7607 (1997).
- ²⁵S. Veliah, R. Pandey, Y. S. Li, and J. M. Newsam, *Chem. Phys. Lett.* **235**, 53 (1995).
- ²⁶F. Calvo, *Phys. Rev. B* **67**, 161403 (2003).
- ²⁷A. Jain, *Comput. Mater. Sci.* **36**, 171 (2006).
- ²⁸J. M. Recio and R. Pandey, *Phys. Rev. A* **47**, 2075 (1993).
- ²⁹J. M. Recio, R. Pandey, A. Ayuela, and A. B. Kunz, *J. Chem. Phys.* **98**, 4783 (1993).
- ³⁰M.-J. Malliavin and C. Coudray, *J. Chem. Phys.* **106**, 2323 (1997).
- ³¹E. de la Puente, A. Aguado, A. Ayuela, and J. M. Lopez, *Phys. Rev. B* **56**, 7607 (1997).
- ³²M. Gutowski, P. Skurski, X. Li, and L. S. Wang, *Phys. Rev. Lett.* **85**, 3145 (2000).
- ³³G. Bilalbegović, *Phys. Rev. B* **70**, 045407 (2004).
- ³⁴D. M. Deaven and K. M. Ho, *Phys. Rev. Lett.* **75**, 288 (1995).
- ³⁵B. Wang and S. Nagase, *J. Phys. Chem. C* **111**, 4956 (2007).
- ³⁶B. L. Wang and S. Y. Yin, *Phys. Rev. Lett.* **86**, 2046 (2001).
- ³⁷J. H. Holland, *Adaptation in Natural and Artificial Systems* (The University of Michigan Press, Ann Arbor, 1975).
- ³⁸J. Carrasco, *Phys. Rev. Lett.* **99**, 235502 (2007).
- ³⁹B. Delly, *J. Chem. Phys.* **92**, 508 (1990).
- ⁴⁰J. P. Perdew and Y. Wang, *Phys. Rev. B* **45**, 13244 (1992).
- ⁴¹Y. Wang and J. P. Perdew, *Phys. Rev. B* **43**, 8911 (1991).
- ⁴²X. D. Gao, X. M. Li, and W. D. Yu, *J. Phys. Chem. B* **109**, 1155 (2005).
- ⁴³Z. W. Pan, Z. R. Dai, and Z. L. Wang, *Science* **291**, 1947 (2001); X. D. Bai, P. X. Gao, and Z. L. Wang, *Appl. Phys. Lett.* **82**, 4806 (2003).
- ⁴⁴C. L. Jiang, W. Q. Zhang, and G. F. Zou, *J. Phys. Chem. B* **109**, 1361 (2005).
- ⁴⁵X. Y. Kong and Z. L. Wang, *Nano Lett.* **3**, 1625 (2003).
- ⁴⁶X. Y. Kong, Y. Ding, R. S. Yang, and Z. L. Wang, *Science* **303**, 1348 (2004).
- ⁴⁷W. L. Hughes and Z. L. Wang, *J. Am. Chem. Soc.* **126**, 6703 (2004).
- ⁴⁸P. X. Gao, Y. Ding, W. J. Mai, W. L. Hughes, C. S. Lao, and Z. L. Wang, *Science* **309**, 1700 (2005).
- ⁴⁹E. C. Behrman, J. R. Myers, and B. R. French, *Phys. Rev. A* **49**, R1542 (1994).
- ⁵⁰M. E. Zandler and E. C. Behrman, *THEOCHEM* **362**, 215 (1996).